


AUTHOR QUERY FORM

	Journal: SIGPRO Article Number: 3998	Please e-mail or fax your responses and any corrections to: E-mail: corrections.esch@elsevier.macipd.com Fax: +44 1392 285878
---	---	--

Dear Author,

Any queries or remarks that have arisen during the processing of your manuscript are listed below and highlighted by flags in the proof. Please check your proof carefully and mark all corrections at the appropriate place in the proof (e.g., by using on-screen annotation in the PDF file) or compile them in a separate list.

For correction or revision of any artwork, please consult <http://www.elsevier.com/artworkinstructions>.

Articles in Special Issues: Please ensure that the words ‘this issue’ are added (in the list and text) to any references to other articles in this Special Issue

Uncited references: References that occur in the reference list but not in the text – please position each reference in the text or delete it from the list.		
Missing references: References listed below were noted in the text but are missing from the reference list – please make the list complete or remove the references from the text.		
Location in article	Query/remark Please insert your reply or correction at the corresponding line in the proof	
	No queries	

Electronic file usage

Sometimes we are unable to process the electronic file of your article and/or artwork. If this is the case, we have proceeded by:

☐ Scanning (parts of) your article
 ☐ Rekeying (parts of) your article
 ☐ Scanning the artwork

Thank you for your assistance.



Contents lists available at ScienceDirect

Signal Processing

journal homepage: www.elsevier.com/locate/sigpro

Effect of offline Rayleigh fading on non-coherent sequence synchronization for multi-user chaos based DS-CDMA

R. Vali *, S.M. Berber, S.K. Nguang

Department of Electrical and Computer Engineering, The University of Auckland, New Zealand

ARTICLE INFO

Article history:

Received 12 August 2009

Received in revised form

16 November 2009

Accepted 21 December 2009

Keywords:

Chaotic sequence synchronization

Fading

Acquisition

Tracking

ABSTRACT

This paper presents the theoretical analysis and simulation results of the effects of frequency flat fading on non-coherent synchronization of a chaos-based DS-CDMA system. The quality of synchronization, both in acquisition and tracking stages, is evaluated in the presence of noise, inter-user interference and fading. This is the first time that a chaotic pilot is used for a non-coherent synchronization block giving it both security (complete signal masking including pilot) as well as usability in low SNRs. There is close agreement between the derived analytical upper bound results in the presence of fading and the simulation results. It is shown in theoretical analysis and simulation that the error output of the tracking loop can be approximated to a Gaussian distribution. Two chip waveforms have been investigated for non-coherent tracking and noise performance of the tracking phase is simulated. The bit error rate of a DS-CDMA system with a chaotic pilot is then investigated in the presence of noise and fading. The effect of partial (worst case) synchronization in terms of SNR difference is then evaluated to be 1 dB for the noise only case, 0.1 dB for single user case with uncompensated fading and 1.1 dB for the eight user case.

© 2010 Published by Elsevier B.V.

1. Introduction

Ever since their introduction to digital communications, chaotic signals have been a subject for active research. The reason for such a high interest stems from them satisfying the three aspects of secret communication set out by Shannon which are concealment, privacy and encryption in physical layer [1–3]. Moreover, the hypersensitivity of chaotic signals to their initial condition is utilized to generate unique orthogonal sequences [2,4]. The sharp shape of the auto-correlation function (ideally a delta function) and small value of cross-correlation function for some chaotic sequences has given rise to the idea of multi-user chaos-based DS-CDMA communication system [2,5–8]. Studies into the suitability of chaotic sequences for spreading purposes in DS-CDMA

have been carried out in [3,9–22] and it was found in [3,9,11,12,14–17,20–22] that suitably chosen chaotic sequences can be used in robust multi-user DS-CDMA systems. Chaotic sequences are also shown to improve the system performance compared to the classical pseudo random binary sequences (PRBS), Gold codes and m sequences [20,23]. Also, in the context of the maximum error free transmission rate, it is shown in [3,18,19] that chaotic sequences perform better than classical spreading sequences.

A DS-CDMA system requires that the transmitter and receiver spreading waveforms be synchronized. If the two waveforms are out of synchronization by as much as one chip duration, the amount of energy reaching the receiver will be proportional to the cross-correlation value which is not sufficient for reliable message detection [24,25]. Acquiring synchronization, that is accurately estimating the time offset between transmitter and receiver, is a difficult problem in low signal to noise ratio (SNR) environments. Moreover, maintaining the acquired

* Corresponding author.

E-mail address: rval013@aucklanduni.ac.nz (R. Vali).

synchronization is also difficult because of various impediments such as clock drift between the transmitter and receiver, channel timing jitter and multipath fading [24,25].

The problem of synchronization for classical multi-user DS-CDMA systems has been addressed in [24–30] and various techniques have been offered. Broadly speaking, the sequence synchronization process can be subdivided into two distinct phases. The first phase is named acquisition which entails determination of an initial timing offset estimate between the transmitted signal and its locally generated replica at the receiver [24–30]. The accuracy of this initial offset estimate has to be within the duration of one chip which is the constituent member of the spreading sequence. In order to achieve initial offset estimate several methods have been proposed in literature, the most popular by far is searching through all the possible delays of a pilot sequence. Naturally this search strategy will have a larger uncertainty if the pilot sequence length is longer which in turn increase the amount of time required for the acquisition phase, therefore the periodicity of the pilot sequences is an essential factor in obtaining synchronization [15,24–26,30,31].

Once the acquisition phase is successfully completed the second phase of the synchronization process, the tracking phase, is started. The aim of the tracking phase is to perform fine synchronization within a fraction of a chip duration as well as maintaining synchronization which might be lost because of noise, channel timing jitter and the relative clock drift between the transmitter and receiver oscillators. The tracking phase is usually implemented in the form of a delay lock loop (DLL) which in principle works similar to a **phase lock loop** (PLL) employed in classical carrier recovery circuits [24,26,30,32].

Chaos-based DS-CDMA systems are no exception to the synchronization requirement and synchronizing chaotic sequences has been an active area of research ever since the idea of chaotic attractor synchronization was first introduced by Yamada and Fujisaka in [33] and was further pursued and put into a secret communication context by Pecora and Carroll in [34,35]. After these pioneering works, many papers have been published dedicated to the subject of chaotic synchronization including the use of Lyapunov's direct method or by using the conditional Lyapunov's exponents [5,36–43].

Since chaotic signals exhibit orthogonality properties that are desirable for DS-CDMA systems, the synchronization techniques of DS-CDMA systems have the potential to be used in the chaotic communication systems [9–11,14–16,44–50]. However, since the correlation properties of chaotic sequences are not analytically obtainable, their performance for synchronization has to be thoroughly investigated. Also, most of the cases in which synchronization of chaotic sequences with classical DS-CDMA techniques have been analyzed, only the acquisition phase is investigated [9–11,14,15,46,48,51,52]. Mazzini et al. in [9,10] have investigated the acquisition of chaotic sequences and has reported that Bernoulli and tailed shift chaotic maps can outperform m and Gold sequences in the

context of code acquisition. However, the tracking procedure has not been examined thoroughly in that investigation. In [9,10,53,54], it has been assumed that no noise exists in the communication channel in order to examine the effects of inter-user interference on the system. However, all multi-user systems have to be robust in the presence of noise which is an ever present phenomenon in communication systems. Markovian chaotic sequences, their generation, bit error rate, code acquisition and **self-interference** have been investigated in [14,22,47,48,51,55] and the potential of such sequences for DS-CDMA applications have been demonstrated; however, none of **these** investigations, consider the tracking problem. The authors in [56] have introduced a type of detection which is achieved by combining a method from optimization theory with the chaotic synchronization theory. Adaptive methods are also in existence but only for PN sequences, a very good example can be found in [57]. Also there is a research gap for evaluation the synchronization performance of chaotic sequences when multipath fading is present.

Recently a synchronization block using classical PRBS within a chaos based DS-CDMA system was suggested in [58] and the orthogonality between chaotic sequences generated from the logistic map time series and PRBS was **utilized** in the form of assigning the PRBS to be the pilot for the synchronization purposes. Further improvements and more detailed implementation issues were addressed in [59] as well as a multiplicative approach for the code assisted pilot. Although PRBS is used as the pilot sequence in [58] it has also been demonstrated that the PRBS pilot does not give any significant advantage in the acquisition quality of synchronization when the logistic map is used as the users' spreading sequence even when there is a significant number of users in the system. A synchronization block with a chaotic pilot on the other hand, has the benefit of being masked completely, since all the signals being broadcast are chaotic, and being simpler because there is no need to have a separate PRBS generator both in the transmitter and receiver. In fact the main advantage of chaos-based DS-CDMA systems lie with the ability of chaotic sequences to mask the information being sent hence keeping it hidden. If a PRBS pilot is used, this advantage will be neutralized. The theoretical analysis for a classical synchronization block utilizing a chaotic pilot has been given in [60]. Additionally, [58] presents a non-coherent acquisition phase which effectively eliminates the carrier phase difference in the system; however, the tracking phase presented in that contribution is coherent, meaning that it needs the carrier phase difference in order to perform tracking. This inconsistency is addressed in the present contribution, by introducing a chaos-based non-coherent tracking loop which has not been addressed in the literature before.

The existing wireless communications systems based on chaotic DS-CDMA are characterized by **the** presence of noise and fading in their channels. The present contribution expands the theoretical analysis of the chaos-based acquisition phase given in [58] to include the multi-path fading phenomenon, which like noise, is always present in the communication channel and has not been addressed

in the context of the chaotic signal acquisition and tracking for DS-CDMA systems.

The rest of this contribution is structured as follows. Section 2 presents a complete non-coherent chaos based DS-CDMA system, with the synchronization block using a chaotic pilot in the presence of noise and fading. This section explains the interactions of the two parts of the synchronization block with the rest of the receiver. Section 3 presents the theoretical analysis related to the chaotic sequence acquisition in the presence of noise and fading as well as numerical results. Section 4 presents the theoretical analysis of the chaos-based non-coherent tracking loop in the presence of noise and fading, a brief discussion about the effect of pulse shaping in the operation of the loop and numerical results. Section 5 presents the overall performance of the chaos-based system in the presence of noise and fading when the non-coherent chaos-based tracking loop is used. The final section is dedicated to conclusions and discussion.

2. The chaotic communication system with the non-coherent synchronization unit in the presence of noise and fading

Fig. 1a shows the chaos-based DS-CDMA system that was introduced in [23] and later used in [58]. Although only the synchronization block is the matter of discussion here, the system is briefly explained assuming that the synchronization process is achieved by the synchronization block on the lower side of the receiver. The transmitter side in Fig. 1a shows the users' messages, that are binary and PNRZ encoded (γ_i^g), being spread using the chaotic spreading sequences x_i^g where $g = 1, 2, 3 \dots N$ and N is the number of users. Each message bit is spread using a certain number of chaotic values known as chips. The number of chips used to spread each bit is known as the spreading factor and will be denoted by 2β from now on. It is also shown that x_i^0 is used for the pilot signal and that γ_i^0 is a continuous stream of +1s. The resulting signal for each user is S_i^g which is summed across all users and the pilot making up the signal which is then filtered, up converted and transmitted. The noisy, faded and delayed version of the transmitted signal reaches the receiver and, provided that the synchronization is achieved, can be down converted, filtered and de-spread using the locally generated replica codes for every users' message by the process of correlation. The correlators generate a +1 if the output is positive and a -1 if the output at the sampling instant is negative. The ± 1 s are the estimates of the transmitted messages for each user denoted by $\hat{\gamma}_i^g$.

The reception quality is dependent on the SNR, the power of fades and the synchronization quality in the channel. The fading phenomenon is modeled statistically as a Rayleigh distributed random variable which affects all the users' sequences as well as the pilot signal; also, the fading coefficient is fixed for a bit period, that is, the fading duration is considered to be as long as a bit duration. It is assumed that the receiver has the initial condition of each of the users available and that the phase difference between the received carrier and locally

generate carrier is eliminated. It is also assumed that the users will begin their transmission at the beginning of the pilot sequence.

In order to keep the consistency of the results, and simplifying the problem, a type of Chebychev polynomial also known as the logistic map is used. The time series for this chaotic map can be generated by

$$x_{n+1}^g = 1 - (2x_n^g)^2. \quad (1)$$

The cross-correlation and auto-correlation properties of this type of map can be found in [61]. It suffices to mention that the time series output of this map is suitably orthogonal for the purposes of the present contribution. The pilot sequence used here is also generated from the same map eliminating the need for a separate spreading code generator. Moreover, the orthogonal sequences can be generated by this map by changing the initial condition by a very small increment.

3. Code acquisition with multi-path fading

This section is concerned with the first phase of the spreading sequence synchronization known as acquisition phase in the presence of noise and slow frequency flat Rayleigh fading. The noise only case is presented in [60] and some analysis with a PRBS pilot is included in [58]. In this section the acquisition phase is analyzed in the presence of fading, the governing equations are then derived and the theoretical results are compared with the simulation results.

3.1. Theoretical framework of the acquisition phase

Fig. 1b shows the circuitry and interconnections of the acquisition and tracking phase of the synchronization block. The tracking phase will be analyzed in Section 4. The acquisition phase is shown on the top part of Fig. 1b. The mathematical model adopted is for bandpass since this is the standard method of analyzing such techniques [24,26,30].

From Fig. 1a we can see that the received signal may be expressed as

$$r_{rec} = a_t \left(\sum_{g=0}^N \gamma_i^g x_i^g \right) \sqrt{2} A \cos(\omega_c t + \phi) + \xi_t(t), \quad (2)$$

where N is the number of users using the channel at the same time, γ_i is the user data, x_i is the chaotic spreading code, A is the pilot amplitude, ω_c is the angular frequency of the carrier, ϕ is the phase shift between the transmitter and receiver, $\xi_t(t)$ is the noise component and a_t is the fading coefficient that characterizes fading influence of the channel on the received signal. a_t has a Rayleigh distribution given by

$$f_a(a) = \frac{a}{b^2} \exp\left(-\frac{a^2}{2b^2}\right), \quad (3)$$

where b is the norm of the Rayleigh distribution whose value is chosen such that the expected value of the fade power equals unity, that is $E[a^2] = 1$.

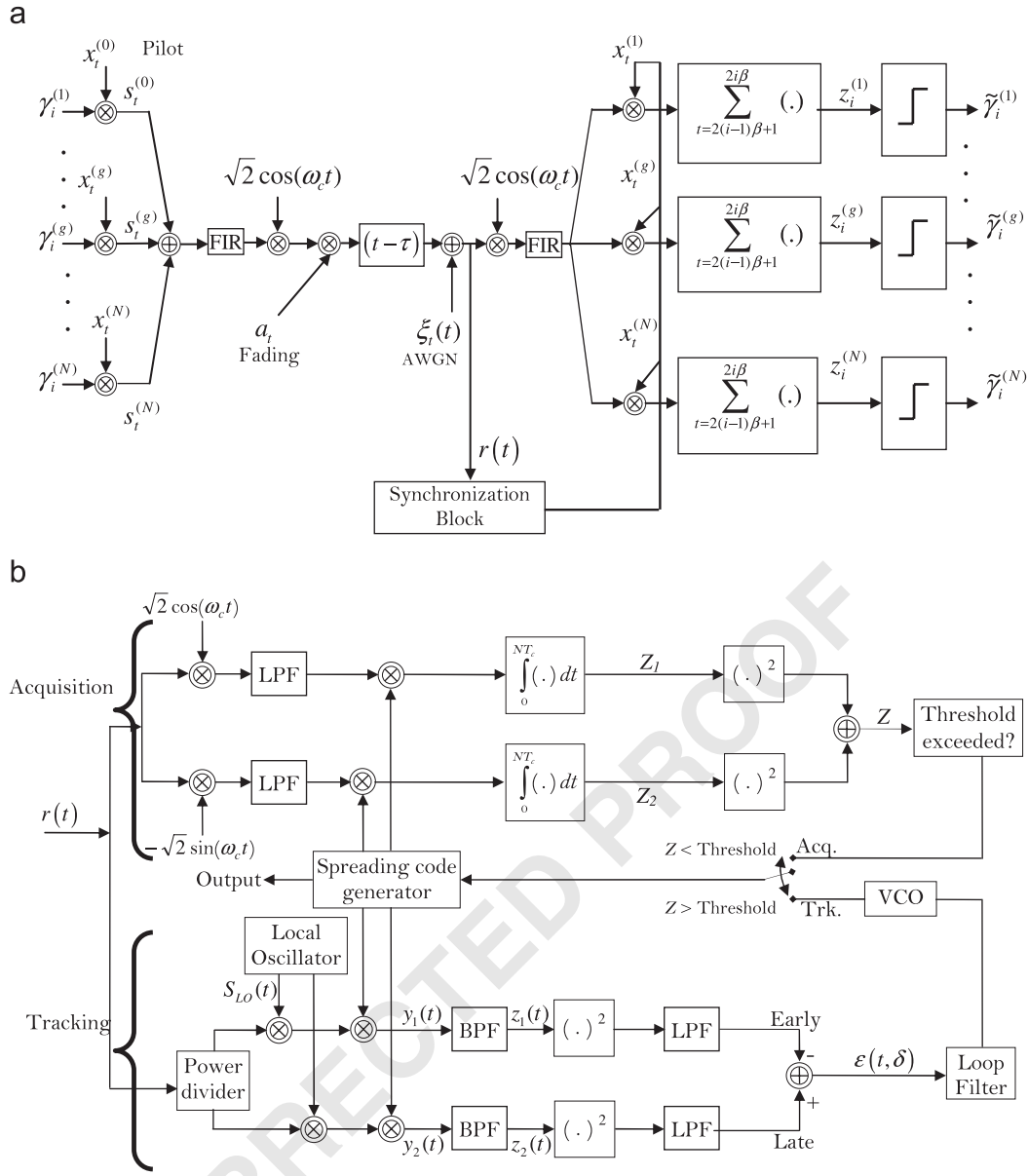


Fig. 1. (a) Chaos based CDMA system. (b) Non-coherent acquisition and tracking.

After demodulation (multiplication with $\cos(\omega_c t)$ and $\sin(\omega_c t)$ and low pass filtering), we can express the outputs of the in phase branch of the demodulator as

$$r_1 = a_t \left(\sum_{g=0}^N \gamma_i^g x_i^g \right) \text{Acos}(\phi) + \zeta_t^I(t) = a_t \gamma_i^0 x_i^0 \text{Acos}(\phi) + a_t \left(\sum_{g=1}^N \gamma_i^g x_i^g \right) \text{Acos}(\phi) + \zeta_t^I(t), \quad (4)$$

where x_i^0 is the chaotic spreading code for the pilot which consists of a certain number of chips and is periodic, γ_i^0 is the pilot data. The period of the pilot sequence is several times that of the spreading factor. The pilot period has a direct relationship to the range of delays that can be

estimated by the system. $\zeta_t^I(t)$ is the in phase component of noise after filtering.

Similarly

$$r_2 = a_t \left(\sum_{g=0}^N \gamma_i^g x_i^g \right) \text{Asin}(\phi) + \zeta_t^Q(t) = a_t \gamma_i^0 x_i^0 \text{Asin}(\phi) + a_t \left(\sum_{g=1}^N \gamma_i^g x_i^g \right) \text{Asin}(\phi) + \zeta_t^Q(t), \quad (5)$$

where $\zeta_t^Q(t)$ is the quadrature component of noise after filtering. We know that the data pilot is always one, i.e. $\gamma_i^0 = 1$, therefore

$$r_1 = a_t x_i^0 \text{Acos}(\phi) + a_t \left(\sum_{g=1}^N \gamma_i^g x_i^g \right) \text{Acos}(\phi) + \zeta_t^I(t). \quad (6)$$

This expression and its quadrature equivalent will be correlated by an m -bit reference sequence containing M chips. This sequence is the same as the transmitter pilot sequence, however, there is a time shift between the two. The time shift directly represents the delay between the transmitter and receiver and the role of acquisition phase is to estimate this time delay. The time delay is expressed as τ .

The correlation result is expressed as

$$\begin{aligned} Z_1 = & A \cos(\phi) \int_{t=0}^{t=MmT_c} \sum_{j=1}^m a_j x_j(t-\tau) x_j(t) dt \\ & + A \cos(\phi) \int_{t=0}^{t=MmT_c} \sum_{j=1}^m \sum_{g=1}^N a_j (\gamma_i^g x_i^g)_j x_j(t-\tau) dt \\ & + \int_{t=0}^{t=MmT_c} \zeta_t^I(t) x(t-\tau) dt. \end{aligned} \quad (7)$$

The second and third lines of Eq. (7) are the interference and noise parts, respectively, and they constitute a random term which will be denoted with RT from now on.

As can be seen from above, the correlation period is divided into m equal sections each consisting of one bit. a_t has been replaced by a_j because a_t denotes a random variable with a Rayleigh distribution that varies with time and a_j is a single sample of that variable acting as a coefficient for one bit period of the transmitted pilot signal. The faded pilot signal is now used to calculate the correlation. Also $x_j(t-\tau)$ and $x_j(t)$ are the j th bits of the correlation period.

In order to continue a statistical characterization of the correlator output (Z_1) has to be performed. The same characterization will apply for the output of the other branch (Z_2). Once these two variables are statistically characterized in the presence of fading, then relevant performance measures for the acquisition scheme can be analytically expressed.

3.1.1. Statistical characterization of fading in acquisition phase

Z_1 can be formulated as

$$\begin{aligned} Z_1 = & C \int_{t=0}^{t=MmT_c} [a_1 x_1(t-\tau) x_1(t) + a_2 x_2(t-\tau) x_2(t) \\ & + \dots + a_m x_m(t-\tau) x_m(t)] dt + RT, \end{aligned} \quad (8)$$

where C is $A \cos(\phi)$.

After expansion we have

$$\begin{aligned} Z_1 = & Ca_1 \int_0^{mT_c} x_1(t-\tau) x_1(t) dt + Ca_2 \int_{mT_c+1}^{2mT_c} x_2(t-\tau) x_2(t) dt \\ & + \dots + Ca_m \int_{(M-1)mT_c+1}^{MmT_c} x_m(t-\tau) x_m(t) dt + RT = Ca_1 R_1(\tau) \\ & + Ca_2 R_2(\tau) + \dots + Ca_m R_m(\tau) + RT. \end{aligned} \quad (9)$$

For a large spreading factor $R_1(\tau) = R_2(\tau) = \dots = R_m(\tau) = R(\tau)$. These terms are correlations over one bit. One complete pilot correlation denoted by $\mathbb{R}(\tau)$ which is the addition of m of the one bit correlations.

Based on the above, Z_1 becomes

$$Z_1 = CR(\tau) \{a_1 + a_2 + \dots + a_m\} + RT = CR(\tau) \sum_{j=1}^m a_j + RT, \quad (10)$$

which is a sum of i.i.d Rayleigh random variables multiplied by constants and added to a random term. Now that the statistical expression for Z_1 is known, the mean and variance for it can be found.

Mean of Z_1 can be found as follows:

$$\begin{aligned} E[Z_1] &= E \left[CR(\tau) \sum_{j=1}^m a_j + RT \right] = E \left[CR(\tau) \sum_{j=1}^m a_j \right] + E[RT] \\ &= CR(\tau) E \left[\sum_{j=1}^m a_j \right] = CR(\tau) m E[a_j] = C \mathbb{R}(\tau) E[a_j] \\ &= C \mathbb{R}(\tau) b \sqrt{\frac{\pi}{2}}, \end{aligned} \quad (11)$$

where $\mathbb{R}(\tau)$ is the complete correlation function over a correlation period, b is the mode of the Rayleigh distribution, and C is a constant and $E[RT] = 0$, because the interference is model led as a zero mean Gaussian random process.

To find the variance of Z_1 we will return to the original expression in Eq. (10). Invoking the central limit theorem we can think of the addition of these random variables to have a Gaussian distribution. Since $E[a_j] = b \sqrt{\pi/2}$ and $\sigma_{a_j}^2 = b^2(2 - \pi/2)$, we will have

$$E[Y] = mb \sqrt{\frac{\pi}{2}}, \quad (12)$$

$$\sigma_Y^2 = mb^2 \left(2 - \frac{\pi}{2} \right). \quad (13)$$

We will focus on Z_1 again

$$Z_1 = CR(\tau)Y + RT = Z_{11} + Z_{12} \quad (14)$$

in which $CR(\tau)Y$ is denoted as Z_{11} and RT is denoted as Z_{12} .

Since Y is a Gaussian distributed random variable, Z_{11} is also a Gaussian distributed random variable. The Z_{11} term is also Gaussian by the virtue of the central limit theorem because it is an addition of several independent identically distributed random variables. We therefore will have

$$\begin{aligned} \sigma_{Z_{11}}^2 &= E[Z_{11}^2] - E^2[Z_{11}] = C^2 R^2(\tau) E[Y^2] - C^2 R^2(\tau) E^2[Y] \\ &= C^2 R^2(\tau) \{E[Y^2] - E^2[Y]\} = C^2 R^2(\tau) \sigma_Y^2 = C^2 R^2(\tau) mb^2 \left(2 - \frac{\pi}{2} \right). \end{aligned} \quad (15)$$

Now we can write down the probability density function of Z_{11} as

$$f_{Z_{11}}(z_{11}) = \frac{1}{\sqrt{2\pi\sigma_{Z_{11}}^2}} \exp \left(-\frac{z_{11} - C \mathbb{R}(\tau) b \sqrt{\frac{\pi}{2}}}{2\sigma_{Z_{11}}^2} \right).$$

For the Z_{12} term we have $E[Z_{12}] = 0$ and $\sigma_{Z_{12}}^2 = N_0 T/2$. N_0 is the sum of the variance of noise (N_0) and the variance introduced by inter-user interference. Therefore for Z_1 we can write down

$$Z_1 = G(E[Z_{11}], \sigma_{Z_{11}}^2 + \sigma_{Z_{12}}^2). \quad (16)$$

If we substitute for the mean and variances we have

$$Z_1 = G \left(C \mathbb{R}(\tau) b \sqrt{\frac{\pi}{2}} C^2 \frac{\mathbb{R}^2(\tau)}{m} b^2 \left(2 - \frac{\pi}{2} \right) + \frac{N_0' T}{2} \right), \quad (17)$$

where we assume that $C^2(\mathbb{R}^2(\tau)/m)b^2(2-\pi/2)+N_0' T/2=N_0'' T/2$ from now on. That is, N_0'' is the sum of the noise, inter-user interference and fading variances all affecting the value of Z_1 .

Because the amplitude of the pilot is $A = \sqrt{2E_c/T_c}$ and the number of chips in the interval T is $M = T/T_c$ we may have

$$\begin{aligned} Z_1 &= G \left(T \sqrt{\frac{2E_c}{T_c}} \cos(\phi) \mathbb{R}(\tau) b \sqrt{\frac{\pi}{2}} \frac{N_0' T}{2} \right) \\ &= \sqrt{\frac{N_0' T}{2}} G \left(2 \sqrt{\frac{TE_c}{T_c N_0'}} \cos(\phi) \mathbb{R}(\tau) b \sqrt{\frac{\pi}{2}}, 1 \right) \\ &= \sqrt{\frac{N_0' T}{2}} G \left(2 \sqrt{\frac{ME_c}{N_0'}} \cos(\phi) \mathbb{R}(\tau) b \sqrt{\frac{\pi}{2}}, 1 \right), \end{aligned} \quad (18)$$

similarly

$$Z_2 = \sqrt{\frac{N_0' T}{2}} G \left(2 \sqrt{\frac{ME_c}{N_0'}} \sin(\phi) \mathbb{R}(\tau) b \sqrt{\frac{\pi}{2}}, 1 \right), \quad (19)$$

since $M = T/T_c$.

The decision variable, which controls the synchronization is $Z = Z_1^2 + Z_2^2$ which makes it $\sigma^2 = N_0'' T/2$ times a non-central chi-squared random variable with two degrees of freedom. The non-centrality parameter is

$$\begin{aligned} \lambda &= \left[2 \sqrt{\frac{ME_c}{N_0'}} \cos(\phi) \mathbb{R}(\tau) b \sqrt{\frac{\pi}{2}} \right]^2 + \left[2 \sqrt{\frac{ME_c}{N_0'}} \sin(\phi) \mathbb{R}(\tau) b \sqrt{\frac{\pi}{2}} \right]^2 \\ &= \frac{ME_c}{N_0''} \mathbb{R}^2(\tau) b^2 \pi. \end{aligned} \quad (20)$$

Therefore the PDF of Z is

$$p_z(z) = \left\{ \frac{1}{2\sigma^2} \exp\left(-\frac{1}{2}(\lambda + z/\sigma^2)\right) I_0\left(\sqrt{\frac{\lambda z}{\sigma^2}}\right), z > 0 \right\}, \quad (21)$$

which is a Rice distribution.

Now that we have the Z parameter we can use it to decide if the synchronization procedure was successful or not. We assume that the decision is based on two hypothesis tests namely

$$H_0 : |\tau| > T_c \Rightarrow \mathbb{R}(\tau) \approx 0, \quad N_0'' > N_0,$$

$$H_1 : |\tau| \leq T_c \Rightarrow \mathbb{R}(\tau) > 0, \quad N_0'' \approx N_0. \quad (22)$$

The two PDFs based on these hypotheses are

$$p_z(z|H_0) = \frac{1}{2\sigma^2} \exp\left(-\frac{1}{2}(z/\sigma^2)\right), \quad (23)$$

$$p_z(z|H_1) = \frac{1}{2\sigma^2} \exp\left(-\frac{1}{2}(\lambda + z/\sigma^2)\right) I_0\left(\sqrt{\frac{\lambda z}{\sigma^2}}\right). \quad (24)$$

It is clear that the non-centrality parameter is zero for the first hypothesis and different from zero in the second. The single attempt ($k=1$) false alarm probability is

$$p_F(k=1) = p(Z > z_T | H_0) = \int_{z_T}^{\infty} \frac{1}{2\sigma^2} \exp\left(-\frac{1}{2}(z/\sigma^2)\right) dz$$

$$= \exp\left(-\frac{1}{2}(z_T/\sigma^2)\right), \quad (25)$$

hence the threshold value can be found as

$$z_T = -2\sigma^2 \ln p_F(k=1) = -N_0'' T \ln p_F(k=1), \quad (26)$$

now the single run detection probability can be found as

$$\begin{aligned} p_D(k=1) &= p_D(Z > z_T | H_1) \\ &= \int_{z_T}^{\infty} \frac{1}{2\sigma^2} \exp\left(-\frac{1}{2}(\lambda + z/\sigma^2)\right) I_0\left(\sqrt{\frac{\lambda z}{\sigma^2}}\right) dz. \end{aligned} \quad (27)$$

Using the change of variable $z = x^2 \sigma^2$, the expression changes to

$$p_D(k=1) = \int_{\sqrt{z_T/\sigma^2}}^{\infty} x \exp\left(-\frac{1}{2}(\lambda + x^2)\right) I_0(\sqrt{\lambda} x) dx, \quad (28)$$

which is the Marcum's Q -function, so

$$p_D(k=1) = Q_M(\sqrt{\lambda}, \sqrt{z_T/\sigma^2}). \quad (29)$$

If the H_1 hypothesis is valid then $\mathbb{R}(\tau) > 0$, $N_0'' \approx N_0$ and $\sigma^2 = N_0 T/2$,

$$\lambda = \frac{ME_c}{N_0} \mathbb{R}^2(\tau) b^2 \pi. \quad (30)$$

Inserting expressions from Eqs. (26) and (30) into Eq. (29) results in

$$\begin{aligned} p_D(m=1) &= Q_M\left(b \mathbb{R}(\tau) \sqrt{\frac{2M\pi E_c}{N_0}}, \sqrt{-\frac{N_0'' T \ln p_F(k=1)}{N_0 T/2}}\right) \\ &= Q_M\left(b \mathbb{R}(\tau) \sqrt{\frac{2M\pi E_c}{N_0}}, \sqrt{-\frac{2N_0'' \ln p_F(k=1)}{N_0}}\right). \end{aligned} \quad (31)$$

The upper bound on the detection probability is obtained when the system is in synchronization i.e. when $\mathbb{R}(\tau) \approx \mathbb{R}(0)$, $N_0'' \approx N_0$, so the expression changes to

$$\begin{aligned} p_D(m=1) &\leq Q_M\left(b \sqrt{\frac{2M\pi E_c}{N_0}}, \sqrt{-2 \ln p_F(k=1)}\right) \\ &\approx Q\left(\sqrt{-2 \ln p_F(k=1)} - b \sqrt{\frac{2M\pi E_c}{N_0}}\right). \end{aligned} \quad (32)$$

In the expression above, $Q(\cdot)$ is a Gaussian Q -function that approximates the Marcum's Q function.

If we compare Eq. (32) with the expression for the upper bound of p_D in [60] we can see the effect of fading in the theoretical expression. That is, the theoretical expression has a new variable which is the mode of the Rayleigh random variable used to model the multi-path fading effect. The power of the fades has a direct influence on the receiver operation characteristics (ROC), which is a plot of p_D vs. p_F and is the main tool for observing the quality of acquisition. The ROC curve is presented for various fading powers in the next section.

3.2. Numerical analysis results and comparison

The results presented in this section compare the simulated ROC of the acquisition phase in the presence of fading with the theoretical prediction of Eq. (31). This is performed for various number of users and SNR, using a correlator period of 200 ($M=200$) and a pilot period of

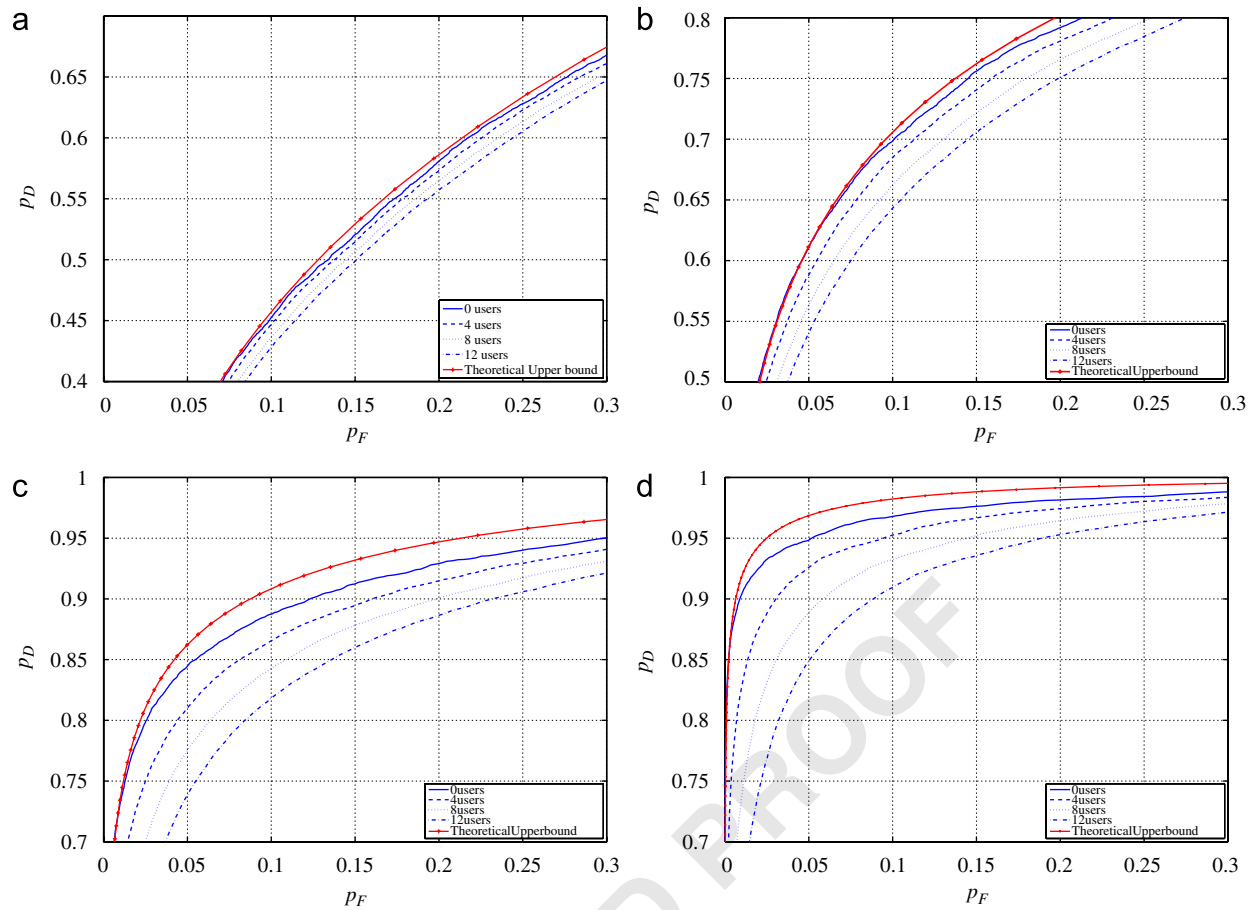


Fig. 2. ROC in the presence of noise (SNR = 0–12 dB), inter-user interference (0–16) and fading ($E[\alpha^2] = 1$), pilot length is 10 times the spreading factor. (a) SNR = 0 dB. (b) SNR = 4 dB. (c) SNR = 8 dB. (d) SNR = 12 dB.

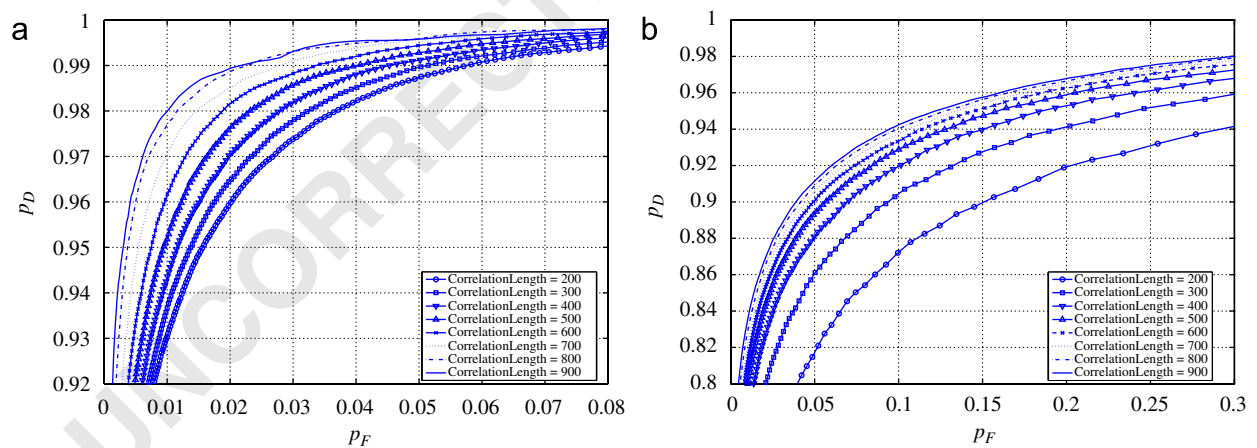


Fig. 3. ROC with different correlation periods, 0 users and SNR of 8 dB: (a) noise and inter-user interference; (b) noise, inter-user interference and fading.

1000 ($mM = 1000$) chips at the average fading power of 1 as explained in Eq. (3). As can be seen from Fig. 2(a) to (d), the simulated ROC in the presence of fading shows a close agreement with the analytical upper-bound predictions of Eq. (32). Also, as expected, the increase in

number of users and noise in the channel decreases the p_D for a fixed p_F . However, the effect of inter-user interference is more pronounced when only noise is present [58]. When fading is present the effect of inter-user interference is reduced and the ROC curves for

different numbers of users come close to each other. This is attributed to the multiplicative effect of fading on the pilot sequence.

Next the ROC when only noise and inter-user interference are present in the channel are shown and compared with the ROC in the presence of fading. As can be seen from Fig. 3, the system performance generally degrades in the presence of deep fades which is expected. The reason is attributed to the multiplicative fading coefficients affecting the auto-correlation peak of the transmitted pilot with its locally generated replica.

It is interesting to observe the effects of increasing the correlation period (M in the theoretical analysis) on the ROC in the presence of fading. In [58] it is shown that the performance of the acquisition phase improves under noise only conditions when the correlation period increases. As shown in Fig. 3 this is also the case when slow flat fading is present in the channel. Increasing the correlation period of the pilot signal improves the ROC only to some extent under fading conditions. There is always some residual decrease in p_D with a fixed p_F value which cannot be overcome with increasing the correlation period. Moreover, increasing the correlation period will increase the acquisition time as the correlator has to perform more computations for each correlation value. An approach that can be used to mitigate the fading effects is the use of interleavers and de-interleavers in the transmitter and receiver, respectively. Using interleaving techniques, the deep fades will be spread across several bit mitigating their effect. This is a subject which is currently under investigation.

4. Non-coherent code tracking

Code tracking is the second stage of the synchronization process for spread spectrum systems. The objective for this stage of the process is to reduce the timing difference remaining between the transmitter and receiver chips [24,26]. Tracking is achieved using phase-locked techniques that are very similar to the ones used to do carrier tracking [24,26]. The chief difference between the carrier tracking loops and modern code tracking loops is in the phase discriminator part. For carrier tracking loops, the phase discriminator can be as simple as a multiplier; however, modern code tracking phase discriminators often make use of multiple correlators and filters [24,26].

Code tracking loops can be categorized into coherent code tracking loops and non-coherent tracking loops. Coherent tracking loops make use of the received carrier phase information. In recent treatments of robust chaotic synchronization for multi-user spread spectrum systems [58,59], it is assumed that the tracking phase is coherent [24,26]. This assumption simplifies the theoretical analysis of the tracking loop for chaotic signals however, there are two major issues in this assumption. The first one is that since the tracking loop input is the spreading code (chaotic spreading code, x_i^s in our case) it must be recovered from the carrier before code tracking. This means that the demodulation process has to be performed before tracking. Because the operational signal to noise

ratio for spread spectrum systems is very low in their transmission bandwidth, the generation of this coherent carrier will be difficult. The second issue is related to the data that the carrier is modulated with. The treatment of tracking phase in [58] and the subsequent structuring work in [59] was performed in base-band, in which the data modulated carrier signal was not present.

Neither of these issues are present for the non-coherent delay lock tracking loop which will be discussed in this paper. The pass-band non-coherent loop proposed here uses the chaotic pilot sequence and has a completely different structure compared to the base-band coherent loop proposed previously in [58]. The discriminator contains two energy detectors which are neither sensitive to carrier data modulation nor carrier phase. The non-coherent chaotic delay lock loop proposed in this section can be used with BPSK. The expansion of this loop to any other modulation scheme is straightforward because the analysis is done with arbitrary data and phase modulation of the carrier.

4.1. Theoretical framework of the tracking phase in the presence of noise and fading

As can be seen from Fig. 1 b the received signal is a carrier which is modulated by data and the delayed spreading code

$$r(t) = a_t \sqrt{2} A x_t^0(t - T_d) \cos(\omega_c t + \gamma_d(t - T_d) + \varphi) + n(t), \quad (33)$$

where A is the amplitude of the received signal, $x_t^0(t - T_d)$ is the delayed pilot chaotic signal in which the delay indicator τ has been replaced with T_d to show that the acquisition phase is now finished and the delays are within the chip duration T_c , ω_c is the carrier angular frequency, $\gamma_d(t - T_d)$ is a delayed arbitrary data phase modulation, φ is the received carrier phase assumed to be random, $n(t)$ is the received noise that is being represented by a band-limited zero mean-WGN process which can be expressed as

$$n(t) = \sqrt{2} n_I(t) \cos(\omega_c t) - \sqrt{2} n_Q(t) \sin(\omega_c t), \quad (34)$$

which has a two sided power spectral density of $N_0/2$ W/Hz. This means that $n_I(t)$ and $n_Q(t)$ are independent zero mean low pass WGN processes.

The multi-path fading effect is expressed by a_t which is the fading coefficient that characterizes fading influence of the channel on the received signal. Fading coefficient a_t has a Rayleigh distribution given by Eq. (3).

As can be seen from Fig. 1 b, the received signal is correlated with the early and late branches of the tracking loop after power division. The output of the reference local oscillator is

$$S_{LO}(t) = \sqrt{2K_1} \cos(\omega_c t - \omega_{IF} t + \varphi'), \quad (35)$$

where K_1 is a gain term, ω_{IF} is the intermediate frequency and φ' is the random phase of the local oscillator. The purpose of the IF bandpass filters shown in Fig. 1 b is to filter out all the sum frequency components that is resulted from the mixing of the power divided received signal with the locally generated spread carrier signal. Therefore, these filters are assumed to have a central

frequency of ω_{IF} and a one sided noise bandwidth of B_N Hertz.

The two outputs of the local carrier spreading are

$$L_1(t) = 2\sqrt{K_1}x_t^0 \left(t - \hat{T}_d + \frac{\Delta}{2}T_c \right) \cos(\omega_c t - \omega_{IF}t + \varphi'), \quad (36)$$

$$L_2(t) = 2\sqrt{K_1}x_t^0 \left(t - \hat{T}_d - \frac{\Delta}{2}T_c \right) \cos(\omega_c t - \omega_{IF}t + \varphi'), \quad (37)$$

where Δ is the time difference between the early and late gates normalized to the chip duration T_c and \hat{T}_d is the estimated time delay [24,26]. Therefore bandpass filter input will be,

$$y_1(t) = L_1(t) \left\{ a_t \sqrt{\frac{A}{2}} x_t^0(t - T_d) \cos(\omega_c t + \gamma_d(t - T_d) + \varphi) + n(t) \right\}, \quad (38)$$

$$y_2(t) = L_2(t) \left\{ a_t \sqrt{\frac{A}{2}} x_t^0(t - T_d) \cos(\omega_c t + \gamma_d(t - T_d) + \varphi) + n(t) \right\}. \quad (39)$$

The inputs to the BPFs are a mixture of signal and noise. In order to simplify the analysis, the signal part is treated separately from the noise part, also, the BPFs are subdivided into a cascade of low-pass and high-pass filters (LPF, HPF) as shown in Fig. 4. The analysis is performed for $x_1(t)$ only as the analysis for $x_2(t)$ is identical.

$y_1(t)$ can be rewritten as

$$y_1(t) = S_1(t) + N_1(t), \quad (40)$$

where

$$S_1(t) = 2a_t A \sqrt{K_1} x_t^0(t - T_d) x_t^0 \left(t - \hat{T}_d + \frac{T_c \Delta}{2} \right) + \cos(\omega_c t + \gamma_d(t - T_d) + \varphi) \times \cos(\omega_c t - \omega_{IF}t + \varphi') \quad (41)$$

and

$$N_1(t) = n_I(t) \cos(\omega_c t) - n_Q(t) \sin(\omega_c t) \times \left\{ 2\sqrt{K_1} x \left(t - \hat{T}_d + \frac{\Delta}{2}T_c \right) \times \cos(\omega_c t - \omega_{IF}t + \varphi') \right\}. \quad (42)$$

This composite signal will go through the BPF which has the **center** frequency ω_{IF} . The bandwidth of the LPF extends from DC to $\omega_{IF} + B_N$ where ω_{IF} is the intermediate frequency on which the BPF is centered and B_N is the filter noise bandwidth. The LPF will exclude all the high frequency components as well as acting as an averaging

integrator if the filter gain is chosen appropriately. The integration time ($T = mMT_c$) is chosen to be much larger than the chip duration (T_c). This means that the signal only output of the LPF is an appropriately scaled integration of the multiplication of two chaotic spreading codes which have a relative time delay that is smaller than a chip duration. The signal part of the output therefore is

$$y_1(t) = \frac{1}{T} \int_0^{mMT_c} S_{1LP}(t) dt, \quad (43)$$

where $S_{1LP}(t)$ is the low pass version of $S_1(t)$ but without the integration. Since $mMT_c = \sum_{k=1}^m kMT_c$, Eq. (43) can be rewritten as

$$z_1(t) = \int_0^{MT_c} a_1 A \sqrt{K_1} x_t^0(t - T_d) x_t^0 \left(t - \hat{T}_d + \frac{T_c \Delta}{2} \right) (\cos(\omega_{IF}t + \varphi - \varphi' + \gamma_d(t - T_d))) dt + \int_{MT_c+1}^{2MT_c} a_2 A \sqrt{K_1} x_t^0(t - T_d) x_t^0 \left(t - \hat{T}_d + \frac{T_c \Delta}{2} \right) (\cos(\omega_{IF}t + \varphi - \varphi' + \gamma_d(t - T_d))) dt + \dots + \int_{MT_c(m-1)+1}^{mMT_c} a_m A \sqrt{K_1} x_t^0(t - T_d) x_t^0 \left(t - \hat{T}_d + \frac{T_c \Delta}{2} \right) (\cos(\omega_{IF}t + \varphi - \varphi' + \gamma_d(t - T_d))) dt. \quad (44)$$

This is a summation of partial correlations of the pilot signal throughout the tracking period scaled by different fading coefficients. So in each complete correlation, fading coefficients with a Rayleigh distribution exist.

The formula above can be expressed as [24,26]:

$$z_1(t) = a_1 A \sqrt{K_1} R_1 \left[\left(\delta + \frac{\Delta}{2} \right) T_c \right] (\cos(\omega_{IF}t + \varphi - \varphi' + \gamma_d(t - T_d))) + a_2 A \sqrt{K_1} R_2 \left[\left(\delta + \frac{\Delta}{2} \right) T_c \right] (\cos(\omega_{IF}t + \varphi - \varphi' + \gamma_d(t - T_d))) + \dots + a_m A \sqrt{K_1} R_m \left[\left(\delta + \frac{\Delta}{2} \right) T_c \right] (\cos(\omega_{IF}t + \varphi - \varphi' + \gamma_d(t - T_d))), \quad (45)$$

where δ is the normalized time difference between the incoming time offset (T_d) and the estimated timing offset (\hat{T}_d), that is $\delta = (T_d - \hat{T}_d)/T_c$.

Since the spreading factor is high, the partial correlations can be assumed to be equal to each other. For

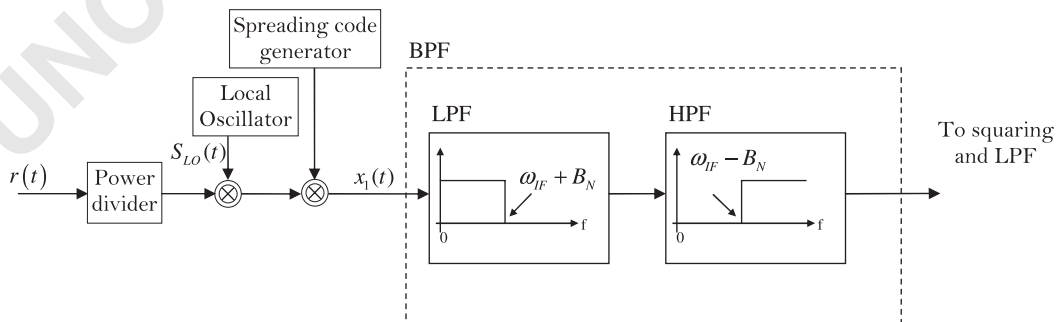


Fig. 4. The tracking loop BPF in detail.

simplicity we assume: $R_1[(\delta + \Delta/2)T_c] = R_2[(\delta + \Delta/2)T_c] = \dots = R_m[(\delta + \Delta/2)T_c] = R[(\delta + \Delta/2)T_c]$.

So the expression for $y_1(t)$ can be simplified to

$$z_1(t) = \sum_{j=1}^m a_j A \sqrt{K_1} R \left[\left(\delta + \frac{\Delta}{2} \right) T_c \right] (\cos(\omega_{IF} t + \varphi - \varphi' + \gamma_d(t - T_d))). \quad (46)$$

The noise part will go through the same BPF as the signal part, in which all the frequencies outside the $\omega_{IF} \pm B_N$ range will be excluded. The noise output of the BPF is the convolution of the noise input with the filter impulse response that is

$$n_1(t) = \int_{-\infty}^{\infty} N_1(t) h(t - \lambda) d\lambda, \quad (47)$$

where $h(t - \lambda)$ is the BPF impulse response at it is assumed that it gives a gain of unity in the $\omega_{IF} \pm B_N$ frequency range. It is shown in literature [24,26] that $n_1(t)$ and $n_2(t)$ are uncorrelated and Gaussian. Therefore, excluding the high frequency components of $N_1(t)$, the noise output of the BPF is

$$n_1(t) = \sqrt{2} \{n_{1I}(t) \cos(\omega_{IF} t) - n_{1Q}(t) \sin(\omega_{IF} t)\}. \quad (48)$$

Similarly the output of the BPF with the input $N_2(t)$ is

$$n_2(t) = \sqrt{2} \{n_{2I}(t) \cos(\omega_{IF} t) - n_{2Q}(t) \sin(\omega_{IF} t)\}. \quad (49)$$

The input to the loop filter is the squared and low pass filtered output of the two BPFs in the early and late branches. Therefore the error signal is [24,26]

$$\varepsilon(t, \delta) = [z_2(t)]_{LP}^2 - [z_1(t)]_{LP}^2, \quad (50)$$

where $z_2(t) = y_2(t) + n_2(t)$ and $z_1(t) = y_1(t) + n_1(t)$.

After expansion and elimination of all double frequency terms

$$\begin{aligned} \varepsilon(t, \delta) = & \frac{1}{2} K_1 A^2 \left(\sum_{j=1}^m a_j \right)^2 \left\{ R^2 \left[\left(\delta - \frac{\Delta}{2} \right) T_c \right] - R^2 \left[\left(\delta + \frac{\Delta}{2} \right) T_c \right] \right\} \\ & + \sqrt{2} K_1 A \left(\sum_{j=1}^m a_j \right) \left\{ R \left[\left(\delta - \frac{\Delta}{2} \right) T_c \right] n_{2I}(t) - R \left[\left(\delta + \frac{\Delta}{2} \right) T_c \right] \right. \\ & n_{1I}(t) \} \times \cos(\varphi - \varphi' + \gamma_d(t - T_d)) \\ & + \sqrt{2} K_1 A \left(\sum_{j=1}^m a_j \right) \left\{ R \left[\left(\delta - \frac{\Delta}{2} \right) T_c \right] \right. \\ & n_{2Q}(t) - R \left[\left(\delta + \frac{\Delta}{2} \right) T_c \right] n_{1Q}(t) \} \times \sin(\varphi - \varphi' \\ & + \gamma_d(t - T_d)) + \{n_{2I}(t)\}^2 + \{n_{2Q}(t)\}^2 - \{n_{1I}(t)\}^2 - \{n_{1Q}(t)\}^2. \end{aligned} \quad (51)$$

The equation above shows the effect of fading on the tracking loop phase discriminator output. If the fading effect is ignored ($a_j = 1$ for all j) then the formula will reduce to the expression given in the literature for the non-coherent tracking loop [24,26].

As can be seen from the equation above, the first line is a DC value which is the desired error function. The rest of the values are low pass filtered signal \times noise and noise \times noise terms. This $\varepsilon(t, \delta)$ will then go through the tracking loop filter which ideally has a bandwidth suitably adjusted to reject nearly all the noise and phase modulated sinusoidal terms. The input to the voltage controlled oscillator is $\frac{1}{2} K_1 A^2 (\sum_{j=1}^m a_j)^2 D_A(\delta)$ where $D_A(\delta)$ is the difference of the

squared values of partial correlation, which is ideally a DC term that is $D_A(\delta) = R^2[(\delta - \Delta/2)T_c] - R^2[(\delta + \Delta/2)T_c]$ [24,26].

If normalized $D_A(\delta)$ is plotted, the resulting curve is known as the tracking loop S-curve which is shown in Fig. 5 and indicated as *Error Signal*. Fig. 5 also shows the squared early, late and on time correlation results as well as the calculated salient points for chaotic signals. According to the authors' knowledge, these salient points have never been presented for chaotic signals before.

The tracking of signal timing is performed by adjusting the speed of the VCO by the amount indicated in the linear region of the S-curve; that is, the most important part of the S-curve is the zero crossing of the Error Signal. In the future section, we attempt to statistically model the effect of noise and fading, in the placement of this zero crossing.

As can be seen from the derivation above, the useful tracking signal (input to the voltage controlled oscillator) can be extracted from the non-coherent chaotic delay lock loop [24,26]. This means that chaotic signals can indeed be tracked non-coherently. This allows us to replace the model presented in [58] which assumes the tracking spreading code to be PRBS with a chaotic spreading code for the tracking phase. The system considered here uses only one spreading code for both acquisition and tracking, minimizes complexity by eliminating the PRBS code generation which is used in [58,59], and increases security of signal transmission.

Before the phase discriminator output can be used for the voltage controlled oscillator, it has to go through the loop filter. The reason is that only the DC part of the signal can be used for tracking the incoming sequence. Therefore in most tracking loops, the loop filter is an averaging integrator which effectively extracts the DC component from Eq. (51).

Assuming the filtering effectively removes the sinusoidal components from Eq. (51), the input to the voltage controlled oscillator is [24,26]

$$\begin{aligned} \varepsilon_{\text{filtered}}(t, \delta) = & \frac{1}{2} K_1 A^2 \left(\sum_{j=1}^m a_j \right)^2 \left\{ R^2 \left[\left(\delta - \frac{\Delta}{2} \right) T_c \right] \right. \\ & \left. - R^2 \left[\left(\delta + \frac{\Delta}{2} \right) T_c \right] \right\} + \{n_{2I}(t)\}^2 + \{n_{2Q}(t)\}^2 - \{n_{1I}(t)\}^2 - \{n_{1Q}(t)\}^2. \end{aligned}$$

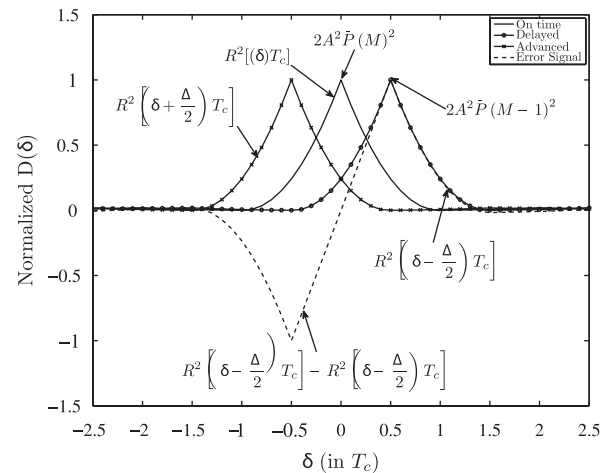


Fig. 5. Tracking loop output for a chaotic pilot when $A = 1$.

4.1.1. Statistical characterization of fading in non-coherent tracking

The input to the voltage controlled oscillator has to be statistically examined. Each a_j is a random variable with a Rayleigh distribution. The noise components ($n_{1I}(t)$, $n_{1Q}(t)$, $n_{2I}(t)$, $n_{2Q}(t)$) are all zero mean random variables with a Gaussian distribution.

The effect of these random variables is examined individually and then the overall effect on the tracking loop is evaluated. Noting that in the operation of the tracking loop, $\sum_{j=1}^m a_j$ is essentially the summation of independent, identically distributed random variables with a Rayleigh distribution since each of the constituents of the summation takes a different random value on every tracking loop trial. Therefore

$$\mu = E \left[\sum_{j=1}^m a_j \right] = mE[a_j] = mb\sqrt{\frac{\pi}{2}}, \quad (52)$$

and

$$\sigma^2 = \text{var} \left[\sum_{j=1}^m a_j \right] = m^2 \sigma_{a_j}^2 = m^2 b^2 \left(2 - \frac{\pi}{2} \right). \quad (53)$$

Using the Central Limit Theorem (CLT), $\sum_{j=1}^m a_j$ is assumed to be a Gaussian distributed random variable with the mean and variance given in the equations above.

As Eq. (51) shows, the desired DC part of the discriminator output is influenced to some degree by the square of the summation of fading coefficients as well as the noise. In order to accurately model the discriminator output statistically, having acquired the distribution of $(\sum_{j=1}^m a_j)$ it is essential to find out the distribution of $(\sum_{j=1}^m a_j)^2$.

It is shown in the above that the distribution of $(\sum_{j=1}^m a_j)$ can be written as:

$$f_g(g) = \frac{1}{\sqrt{2\pi\sigma^2}} \exp \left(-\frac{(g-\mu)^2}{2\sigma^2} \right), \quad (54)$$

where μ and σ^2 are shown in Eqs. (52) and (53), respectively.

If a random variable \mathbb{G} has a Gaussian distribution $f_g(g)$ then the distribution of random variable \mathbb{H} where $\mathbb{H} = \mathbb{G}^2$ is given by a non-central chi-square distribution with one degree of freedom and with a non-centrality parameter of $\lambda = \pi/(4-\pi)$.

The same theory is applied for the Gaussian noise components that are squared in the phase discriminator output expression given above. However, those are chi-square distributions because the noise has a zero mean. They all have one degree of freedom.

The analysis above shows that in the presence of noise and fading, the DC value used for tracking is an addition of five chi-square distributions. Using the CLT again, we speculate that $\varepsilon_{\text{filtered}}(0,0)$ (input to the voltage controlled oscillator), will fluctuate around its mean with a Gaussian distribution.

We will confirm our view by simulating the system and observing the distribution of $\varepsilon_{\text{filtered}}(0,0)$ around the mean.

As can be seen from Fig. 6(a) and (b), the presence of Rayleigh fading does not affect the PDF of $\varepsilon_{\text{filtered}}(0,0)$. This is because of the very small value of $R^2[(\delta - \Delta/2)T_c] - R^2[(\delta + \Delta/2)T_c]$ when $\delta = 0$ which effectively removes the squared sum of fading coefficients. This experiment confirms our theory based assumption that the values of the error on the zero crossing point of the S-curve are going to be normally distributed if there is fading present in the channel.

4.2. Effects of pulse shaping and noise on the tracking loop properties

In order to perform code tracking for DS-CDMA signals, it is necessary to have the notion of a chip duration (T_c in this case), with a sufficiently high resolution so that the tracking phase which is concerned with time delays in the order of a fraction of chip, can perform its task. However, throughout the literature related to the tracking phase of the synchronization block for DS-CDMA systems, it is assumed that the spreading chips keep a constant value over the chip duration (rectangular pulse). The tracking phase error curves presented in [24,30,62] for classical

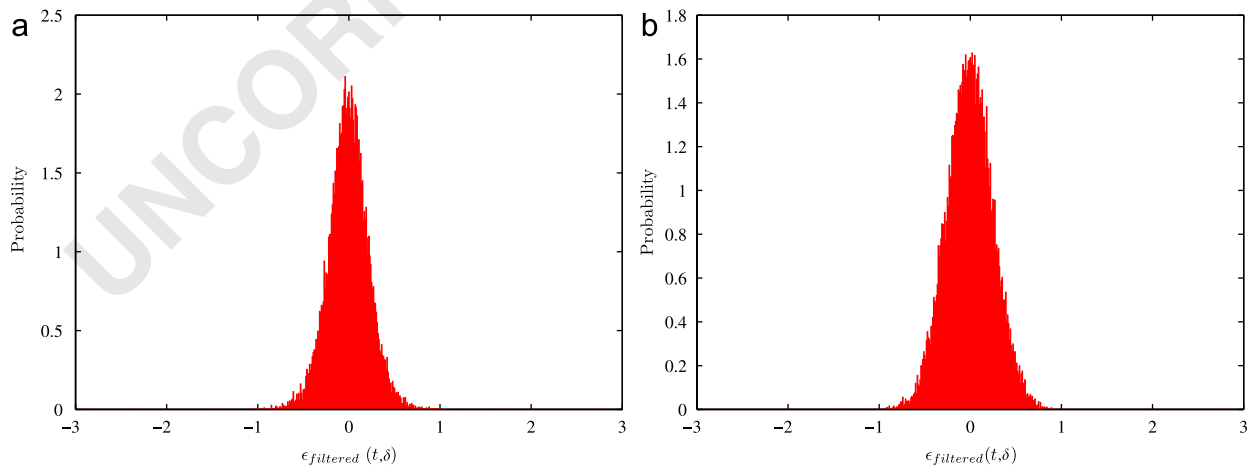


Fig. 6. The PDF of $\varepsilon_{\text{filtered}}(t, \delta)$ at $t = 0$ and $\delta = 0$: (a) the in the presence of noise only and (b) in the presence of noise and fading (SNR = 6 dB both cases).

DS-CDMA and in [58] for the chaos-based case, did not take into account the pulse shaping and filtering that are included in the system. Moreover, rectangular pulses lead to an increase in the transmission bandwidth which is not desirable. In order to address this issue the tracking phase of the synchronization block has been modeled with interpolated chaotic samples that have the same bandwidth as the original un-sampled signal since they have been low pass filtered at the end of the interpolation process. The error curve results for various values of Δ are given in Fig. 7. As can be seen, the pulse shaping has a direct effect on the shape of the errors curves, also, increasing the value of Δ to twice the chip length (Fig. 7 d) will introduce a point with a zero slope. This is highly undesirable because it introduces errors in the tracking process and has to be avoided.

Fig. 8 shows the effect of noise for the two types of pulse shaping used for the tracking loop. As can be seen, the linear region of the loop is affected by noise and it no longer crosses the zero line at the correct time. Noisy conditions introduce errors in the tracking process which could ultimately result in the loss of synchronization.

4.3. Numerical analysis results and comparison for the tracking phase

The non-coherent tracking loop investigated in the previous section is now used for tracking the incoming signal. The cumulative and instantaneous estimations are shown for both noiseless and noisy conditions in Fig. 9. The tracking loop for both cases is set to run for 40 iterations. In the noiseless case, it is evident that the non-coherent tracking loop has an optimal performance because the random jitter (T_d) is tracked for all iterations and each estimation (\hat{T}_d) is the same as the value of jitter for the previous step. In the noisy case, the incoming jitter is not tracked optimally because of the presence of noise which affects the correlation function. As can be seen the cumulative values for T_d and \hat{T}_d diverge. If the difference between the cumulative values becomes more than a chip duration, the acquisition phase has to be restarted as the synchronization is lost. The work presented in [58], only presented the noiseless tracking loop performance which is unrealistic in real communication channels. The figures below, however,

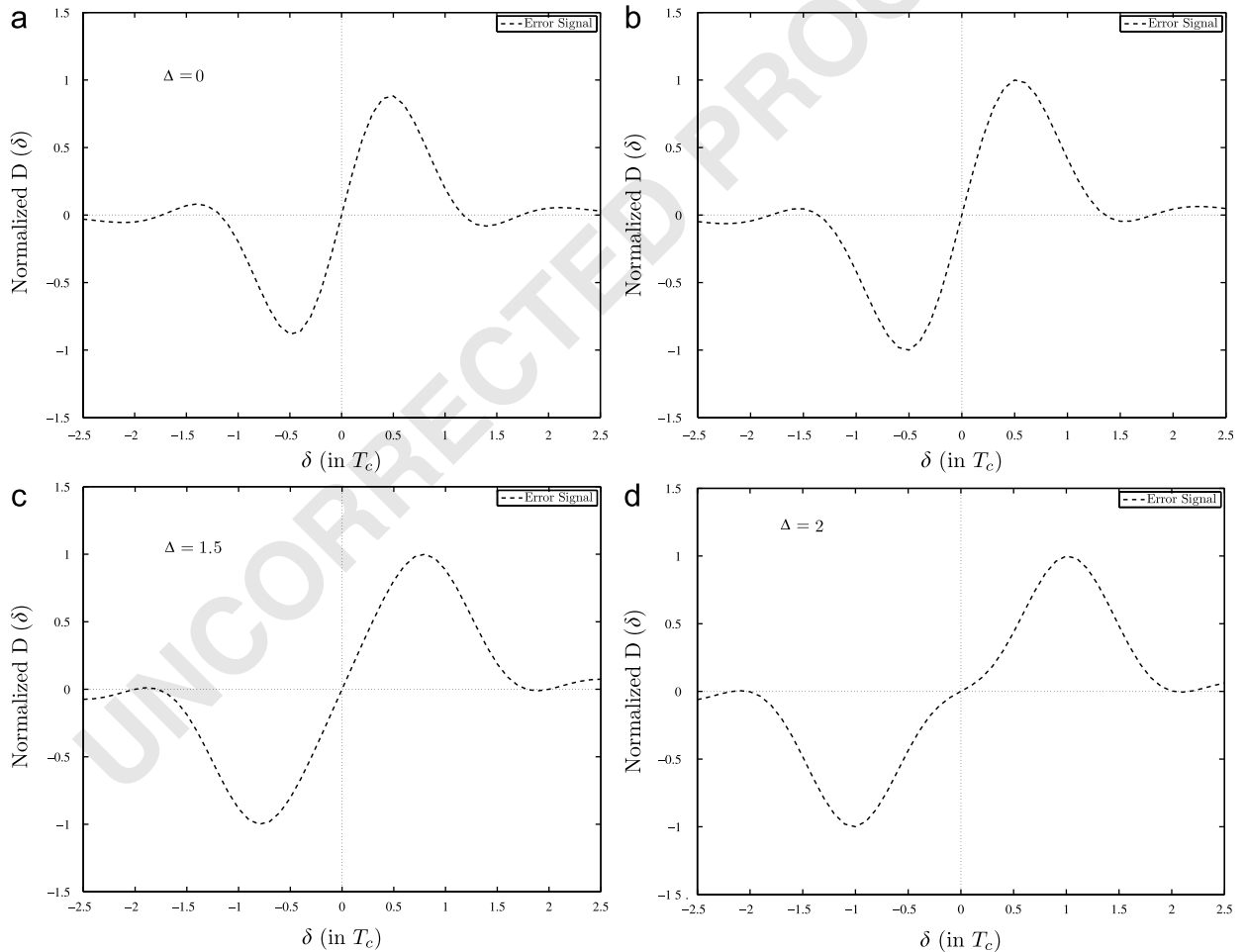


Fig. 7. Non-coherent tracking loop error curves with filtered pulses for different values of Δ .

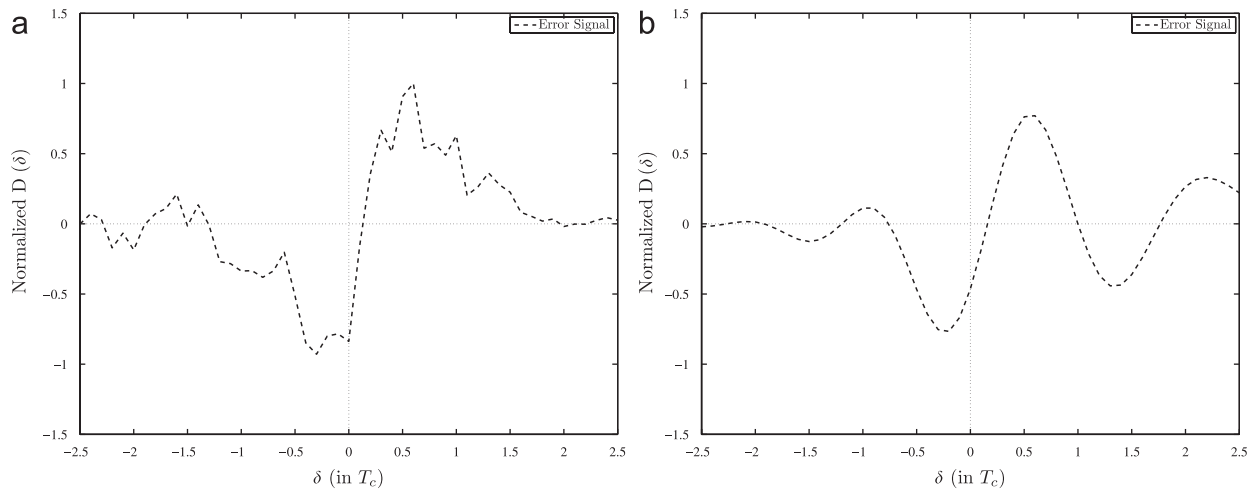


Fig. 8. Tracking loop error signal for (a) noisy rectangular chaotic sequences and (b) noisy interpolated chaotic sequences (SNR = 6 dB both cases).

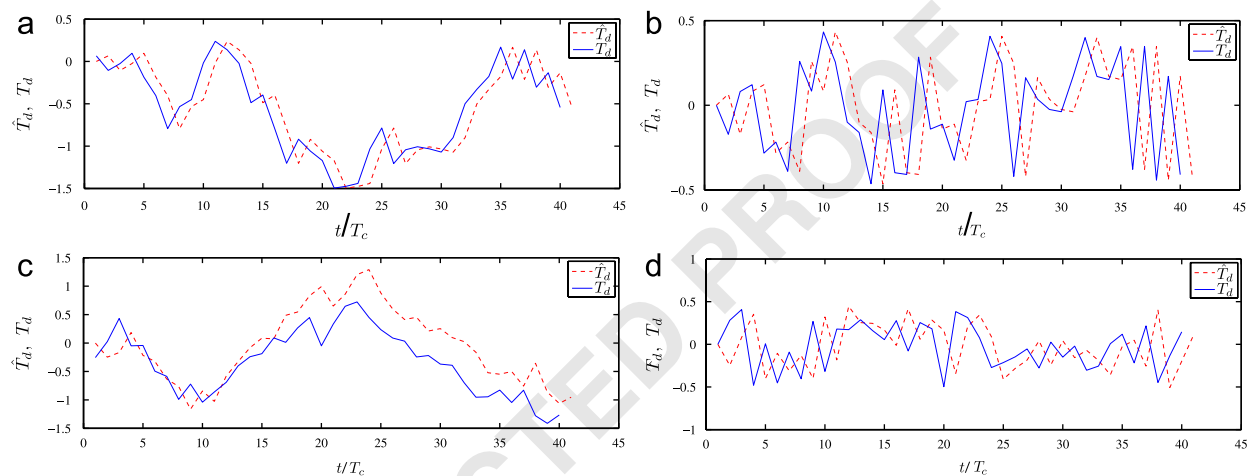


Fig. 9. Timing jitter, T_d and its estimation \hat{T}_d , (a) cumulative values and (b) simultaneous values, (c) and (d) show the same values for a noisy environment (SNR = 8 dB).

show the effect of channel impurities on the actual tracking of signals.

5. Overall system performance evaluation in the presence of fading and synchronization faults

In this section, the overall chaos-based DS-CDMA system performance presented in Fig. 1 a is analyzed. The theoretical probability of error equations for system with noise and inter-user interference are presented in [63] and the equations governing the system performance in a slow frequency flat fading channel is presented in [64]. The equations are repeated here for convenience. The probability of error for the g -th users of the CDMA system when only noise is present is [63]

$$p_g^e = \frac{1}{2} \operatorname{erfc} \left(\left[\frac{\psi + N - 1}{\beta} + \left(\frac{a^2 E_b}{N_0} \right)^{-1} \right]^{-1/2} \right), \quad (55)$$

and the probability of error when fading is present in the channel is [64]

$$p_{\text{Fading}}^e = \int_0^\infty \frac{a}{b^2} \frac{1}{2} \operatorname{erfc} \left(\left[\frac{\psi + N - 1}{\beta} + \left(\frac{a^2 E_b}{N_0} \right)^{-1} \right]^{-1/2} \right) \exp \left(-\frac{a^2}{2b^2} \right) da, \quad (56)$$

where ψ represents the time domain characteristics of the chaotic signals and equals 0.5 for the logistic map, N is the number of users, β is half the spreading factor, E_b is the signal energy per bit, N_0 is the noise power spectral density and a follows the same distribution as Eq. (3).

In both cases, it is assumed that the transmitted signals are perfectly synchronized with the received signals. In Fig. 10, the theoretical curves are drawn using the probability of error equations in [63,64] alongside the simulated curves.

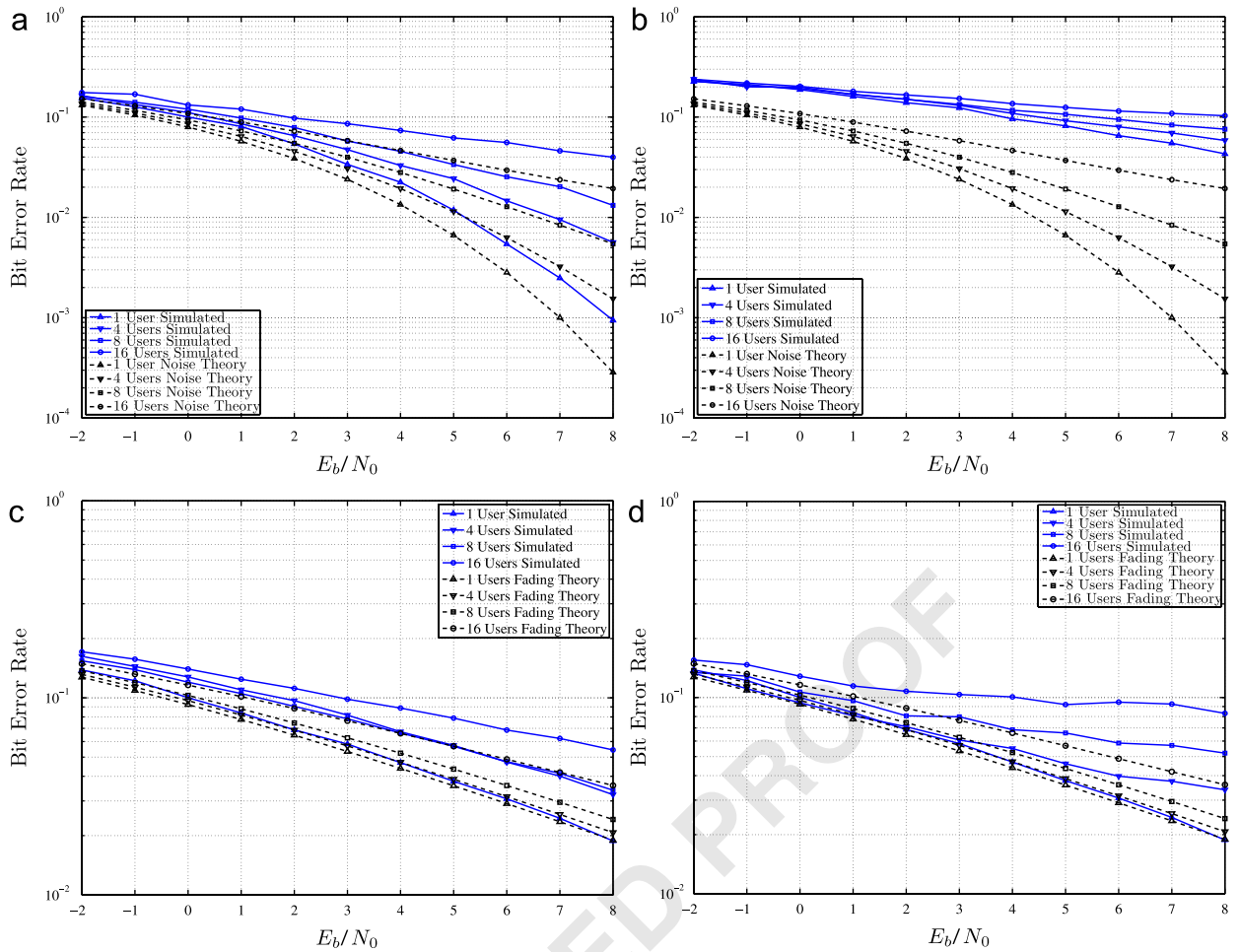


Fig. 10. Simulated BER curves and theoretical probability of error predictions for the CDMA system with partially misaligned chips with the presence of noise, inter-user interference and fading. (a) Misalignment within a chip duration with noise and inter-user interference, (b) misalignment beyond a chip duration with noise and inter-user interference, (c) misalignment within a chip duration with fading and (d) misalignment beyond a chip duration with fading.

It should be noted that Eqs. (55) and (56) are based on Gaussian approximation. Exact BER expressions and derivation for AWGN can be found in [65] and for the m -fading channel in [66].

In the simulations it is assumed that there is some misalignment between the chips in the transmitter and receiver. The misalignment is assumed to be either within a fraction of a chip duration (Fig. 10 a and c) or larger than a chip duration (Fig. 10 b and d). It should be noted that the scenarios presented in Fig. 10 are to show the importance of synchronization in the CDMA system. In reality, the sampling rate of the chips is done in a way that the maximum time difference between the transmitter and receiver is a small fraction of one chip duration. What is shown in the scenarios is the absolute worst case scenario. Also, it should be noted that the flat fading is not compensated by interleavers in the figures shown, which is part of the reason for the increase in the bit error rate. Currently, the usage of interleavers to neutralize the fading issue is under investigation for both non-coherent acquisition and tracking.

6. Conclusions

In this paper it is demonstrated that non-coherent synchronization using a chaotic pilot in the DS-CDMA platform is possible. The mathematical framework for both the non-coherent acquisition and tracking phase is derived in the presence of fading for the first time. A chaos-based acquisition phase is investigated in the presence of noise, inter-user interference and fading. It was found that fading has an adverse effect on the acquisition phase performance and cannot be fully compensated by increasing the pilot correlation period. Also, it is demonstrated that the influence of inter-user interference on the acquisition performance reduces in presence of fading. A chaos-based non-coherent tracking phase is investigated in the presence of noise and fading and usage of two different pulse shaping methods (rectangular and interpolation) are then examined. It is proven both by mathematical analysis and simulation that the effect of fading on the tracking loop error curve can be modeled as a random variable with a Gaussian

distribution. It is demonstrated that noise and fading induce errors in the tracking process which results in the loss of synchronization. The degradation of system performance is then evaluated when the CDMA system is simulated in the presence of noise, inter-user interference and fading. The results are then compared with the theoretical results existing in literature that assume perfect synchronization. It is shown that a misalignment of more than one chip duration between the transmitter and receiver increases the bit error rate to more than the acceptable limit of 10^{-3} .

References

- [1] C.E. Shannon, Communication theory of secrecy systems, Bell Systems Technical Journal 28 (1949) 656–715.
- [2] P. Stavroulakis, Chaos applications in telecommunications, 2006.
- [3] R. Rovatti, G. Mazzini, G. Setti, Shannon capacities of chaos-based and conventional asynchronous DS-CDMA systems over AWGN channels, Electronics Letters 38 (May 2002) 478–480.
- [4] M.P. Kennedy, R. Rovatti, G. Setti, Chaotic Electronics in Telecommunications, CRC Press, Boca Raton, FL, 2000.
- [5] K.M. Cuomo, A.V. Oppenheim, Circuit implementation of synchronized chaos with applications to communications, Physics Review Letters 71 (July 1993) 65–68.
- [6] H. Kamata, T. Endo, Y. Ishida, Secure communication system using chaos via dsp implementation, in: Proceedings of the IEEE International Symposium on Circuits and Systems ISCAS '96, 'Connecting the World', vol. 3, 12–15 May 1996, pp. 112–115.
- [7] G. Kolumban, M.P. Kennedy, L.O. Chua, The role of synchronization in digital communications using chaos, I. Fundamentals of digital communications, IEEE Transactions on Circuits and Systems—Part I: Fundamental Theory and Applications 44 (October 1997) 927–936.
- [8] G. Kolumban, M.P. Kennedy, L.O. Chua, The role of synchronization in digital communications using chaos, II. Chaotic modulation and chaotic synchronization, IEEE Transactions on Circuits and Systems—Part I: Fundamental Theory and Applications 45 (November 1998) 1129–1140.
- [9] G. Mazzini, G. Setti, R. Rovatti, Chaotic complex spreading sequences for asynchronous DS-CDMA. I. System modeling and results, IEEE Transactions on Circuits and Systems—Part I: Fundamental Theory and Applications 44 (October 1997) 937–947.
- [10] G. Setti, R. Rovatti, G. Mazzini, Synchronization mechanism and optimization of spreading sequences in chaos-based DS-CDMA systems, IEEE Transactions on Fundamentals of Electronics, Communications and Computer Sciences E82-A (September 1999) 1737–1746.
- [11] G. Mazzini, R. Rovatti, G. Setti, Sequence Synchronization in Chaos-based DS-CDMA Systems, vol. 4, 1998, pp. 485–488.
- [12] G. Mazzini, R. Rovatti, G. Setti, Chaos-based asynchronous DS-CDMA systems and enhanced rake receivers: measuring the improvements, IEEE Transactions on Circuits and Systems—Part I: Fundamental Theory and Applications 48 (December 2001) 1445–1453.
- [13] G. Setti, R. Rovatti, G. Mazzini, Performance of chaos-based asynchronous DS-CDMA with different pulse shapes, IEEE Communications Letters 8 (July 2004) 416–418.
- [14] T. Kohda, Y. Jitsumatsu, T.A. Khan, Spread-spectrum Markovian-code acquisition in asynchronous DS/CDMA systems, in: Proceedings of the International Symposium on Circuits and Systems ISCAS'03, vol. 3, 25–28 May 2003, pp. III-750–III-753.
- [15] N. Eshima, T. Kohda, Statistical approach to the code acquisition problem in direct-sequence spread-spectrum communication systems, IMA Journal of Mathematical Control & Information 23 (2) (2006) 149–163.
- [16] C.-C. Chen, K. Yao, Design of spread spectrum sequences using chaotic dynamical systems with lebesgue spectrum, in: Proceedings of the IEEE International Symposium on Circuits and Systems ISCAS 2001, vol. 3, 6–9 May 2001, pp. 149–152.
- [17] R. Rovatti, G. Setti, G. Mazzini, Chaotic complex spreading sequences for asynchronous DS-CDMA. Part II. Some theoretical performance bounds, IEEE Transactions on Circuits and Systems—Part I: Fundamental Theory and Applications 45 (April 1998) 496–506.
- [18] R. Rovatti, G. Mazzini, G. Setti, On the ultimate limits of chaos-based asynchronous DS-CDMA-II: analytical results and asymptotics, IEEE Transactions on Circuits and Systems—Part I: Regular Papers 51 (July 2004) 1348–1364.
- [19] R. Rovatti, G. Mazzini, G. Setti, On the ultimate limits of chaos-based asynchronous DS-CDMA-I: basic definitions and results, IEEE Transactions on Circuits and Systems—Part I: Regular Papers 51 (July 2004) 1336–1347.
- [20] G.S.R. Rovatti, G. Mazzini, Chaos-based spreading compared to m-sequences and Gold spreading in asynchronous CDMA communication systems, in: Proceedings of the 1997 European Conference on Circuit Theory and Design, Budapest, Hungary, 1997.
- [21] C.C. Chen, K. Yao, K. Umeno, E. Biglieri, Design of spread-spectrum sequences using chaotic dynamical systems and ergodic theory, IEEE Transactions on Circuits and Systems—Part I: Fundamental Theory and Applications 48 (September 2001) 1110–1114.
- [22] H. Fujisaki, On optimum 3-phase spreading sequences of simple Markov chains, in: Proceedings of the IEEE International Symposium on Circuits and Systems ISCAS 2001, vol. 3, 6–9 May 2001, pp. 229–232.
- [23] U. Parlitz, S. Ergezeinger, Robust communication based on chaotic spreading sequences, Physics Letters A 188 (2) (1994) 146–150.
- [24] R.L. Peterson, R.E. Zeimer, D.E. Borth, Introduction to Spread Spectrum Communication, Prentice-Hall, Englewood Cliffs, NJ, 1995.
- [25] L. Hanzo, L. Yang, E. Kuan, K. Yen, Single and Multi-Carrier DS-CDMA Multi-User Detection, Space-Time Spreading, Synchronisation and Standards, IEEE Press Wiley, Chichester, 2003.
- [26] M.K. Simon, J.K. Omura, R.A. Scholtz, B.K. Levitt, Spread Spectrum Handbook, McGraw-Hill, Inc, 2002.
- [27] S. Haykin, M. Moher, Introduction to Analog & Digital Communications, second ed., Wiley, New York, 2007.
- [28] B.G. Agee, R.J. Kleinman, J.H. Reed, Soft synchronization of direct sequence spread-spectrum signals, IEEE Transactions on Communications 44 (11) (1996) 1527–1536.
- [29] P. Kartaschoff, Synchronization in digital communications networks, Proceedings of the IEEE 79 (7) (1991) 1019–1028 0018-9219.
- [30] J.K. Holmes, Spread Spectrum Systems for GNSS and Wireless Communications, GNSS Technology and Applications, Artech House, London, 2007.
- [31] F. Gardner, A bpsk/qpsk timing-error detector for sampled receivers, IEEE Transactions on Communications [legacy, pre - 1988] 34 (5) (1986) 423–429.
- [32] P. Hyung-Rae, Performance analysis of a decision-feedback coherent code tracking loop for pilot-symbol-aided ds/ss systems, IEEE Transactions on Vehicular Technology 55 (4) (2006) 1249–1258 0018-9545.
- [33] H. Fujisaka, T. Yamada, Stability theory of synchronized motion in coupled-oscillator systems, Progress of Theoretical Physics 69 (1983) 32–47.
- [34] L.M. Pecora, T.L. Carroll, Synchronisation in chaotic systems, Physical Review Letters 64 (February 1990).
- [35] T. Carroll, L. Pecora, Using multiple attractor chaotic systems, in: 1998 IEEE International Conference on for communication, Electronics, Circuits and Systems, vol. 1, 1998, pp. 103–106.
- [36] L.O. Chua, M. Itoh, L. Kocarev, K. Eckert, Chaos synchronization in chua's circuit, Technical Report UCB/ERL M92/111, EECS Department, University of California, Berkeley, 1992.
- [37] A. Oppenheim, G. Wornell, S. Isabelle, K. Cuomo, Signal processing in the context of chaotic signals, in: 1992 IEEE International Conference on Acoustics, Speech, and Signal Processing, ICASSP-92, vol. 4, March 1992, pp. 117–120.
- [38] C. Wu, L.O. Chua, A unified framework for synchronization and control of dynamical systems, Technical Report UCB/ERL M94/28, EECS Department, University of California, Berkeley, 1994.
- [39] U. Parlitz, L. Kocarev, Synchronization of chaotic systems, in: H. Schuster (Ed.), Handbook of Chaos and Control, Wiley-VCH, 1999.
- [40] K. Murali, Heterogeneous chaotic systems based cryptography, Physics Letters A 272 (3) (2000) 184–192.
- [41] L. Kocarev, U. Parlitz, R. Brown, Robust synchronization of chaotic systems, Physical Review 61 (4) (2000).
- [42] J. Lu, X. Wu, J. Lu, Synchronization of a unified chaotic system and the application in secure communication, Physics Letters A 305 (6) (2002) 365–370.
- [43] B. Jovic, S. Berber, C.P. Unsworth, A novel mathematical analysis for predicting master-slave synchronization for the simplest quadratic chaotic flow and UEDA chaotic system with application to

- communications, *Physica D: Nonlinear Phenomena* 213 (1) (2006) 31–50.
- [44] M. Feki, B. Robert, G. Gelle, M. Colas, Secure digital communication using discrete-time chaos synchronization, *Chaos, Solitons & Fractals* 18 (4) (2003) 881–890.
- [45] M. Feki, An adaptive chaos synchronization scheme applied to secure communication, *Chaos, Solitons & Fractals* 18 (1) (2003) 141–148.
- [46] T.A. Khan, N. Eshima, Y. Jitsumatsu, T. Kohda, Multiuser code acquisition in ds/cdma systems, in: *Proceedings of the IEEE Topical Conference on Wireless Communication Technology*, 15–17 October 2003, pp. 121–122.
- [47] Y. Jitsumatsu, T. Kohda, Bit error rate of incompletely synchronised correlator in asynchronous DS/CDMA system using SS Markovian codes, *Electronics Letters* 38 (April 2002) 415–416.
- [48] Y. Jitsumatsu, N. Eshima, T. Kohda, Code acquisition of Markovian SS codes in a chip-synchronous DS-CDMA system, in: *Proceedings of the IEEE International Symposium on Information Theory*, 29 June–4 July 2003, p. 447.
- [49] C.-s. Zhou, T.-l. Chen, Robust communication via chaotic synchronization based on contraction maps, *Physics Letters A* 225 (1–3) (1997) 60–66.
- [50] D.R.D.F.-P.G. Kaddoum, P. Charge, A methodology for bit error rate prediction in chaos-based communication systems, *Circuits, Systems, and Signal Processing* (2009).
- [51] Y. Jitsumatsu, T. Kohda, On the self-interferences of SS codes generated by a Markov chain, in: *Proceedings of the IEEE International Symposium on Information Theory*, 2002, p. 67.
- [52] J.-P. Mangeot, F. Launay, P. Coirault, A multi-user transmission using chaotic carriers, *Communications in Nonlinear Science and Numerical Simulation* 14 (6) (2009) 2709–2719.
- [53] G.S.R. Rovatti, G. Mazzini, Statistical features of chaotic maps related to CDMA systems performance, in: *Proceedings of the 1998 International Symposium on Mathematical Theory of Networks and Systems (MTNS'98)*, 1998.
- [54] G. Setti, G. Mazzini, R. Rovatti, Gaussian characterization of self-interference during synchronization of chaos based DS-CDMA systems, 1998.
- [55] H. Fujisaki, On correlation values of m-phase spreading sequences of Markov chains, *IEEE Transactions on Circuits and Systems—Part I: Fundamental Theory and Applications* 49 (December 2002) 1745–1750.
- [56] D. He, H. Leung, Quasi-orthogonal chaotic cdma multi-user detection using optimal chaos synchronization, *IEEE Transactions on Circuits and Systems—Part II: Express Briefs* 52 (November 2005) 739–743.
- [57] H.-S. Oh, D.-S. Han, An adaptive double-dwell pn code acquisition system in ds-cdma communications, *Signal Processing* 85 (12) (2005) 2327–2337.
- [58] B. Jovic, C. Unsworth, G. Sandhu, S. Berber, A robust sequence synchronization unit for multi-user DS-CDMA chaos-based communication systems, *Signal Processing* 87 (7) (2007) 1692–1708.
- [59] G. Kaddoum, D. Roviras, P. Charge, D. Fournier-Prunaret, Robust synchronization for asynchronous multi-user chaos-based ds-cdma, *Signal Processing* 89 (5) (2009) 807–818.
- [60] S. Berber, B. Jovic, Sequence synchronization in a wideband cdma system, in: *Proceedings of the 2006 International Conference on Wireless Broadband and Ultra Wideband Communications (AusWireless06)*, Sydney, Australia, 13–16 March 2006, pp. 1–6.
- [61] G. Sandhu, S. Berber, Investigation on operations of a secure communication system based on the chaotic phase shift keying scheme, in: *Third International Conference on Information Technology and Applications*, 2005, ICITA 2005, vol. 2, 4–7 July 2005, pp. 584–587.
- [62] J.S. Lee, L.E. Miller, *CDMA Systems Engineering Handbook*, Mobile Communications, Artech House, London, 1998.
- [63] W.M. Tam, F.C.M. Lau, C.K. Tse, A.J. Lawrance, Exact analytical bit error rates for multiple access chaos-based communication systems, *IEEE Transactions on Circuits and Systems—Part II: Express Briefs* 51 (September 2004) 473–481.
- [64] G. Sandhu, S. Berber, Investigation on orthogonal signals for secure transmission in multiuser communication systems, in: *Proceedings of the 2006 International Conference on Wireless Broadband and Ultra Wideband Communications (AusWireless06)*, Sydney, Australia, 13–16 March 2006.
- [65] G. Kaddoum, P. Charge, D. Roviras, A generalized methodology for bit-error-rate prediction in correlation-based communication schemes using chaos, *IEEE Communications Letters* 13 (August 2009) 567–569.
- [66] G. Kaddoum, M. Coulon, D. Roviras, P. Charge, Performance of multi-user asynchronous chaos-based communication systems through m-distributed fading channel, in: *Proceedings of the 17th European Signal processing Conference, EUSIPCO 2009*, Glasgow, Scotland, 24 August 2009.